

Burst Mechanisms in Hydrodynamics

E. Knobloch & J. Moehlis

Department of Physics, University of California,

Berkeley, CA 94720, USA

E-Mail: knobloch@physics.berkeley.edu

Abstract

Different mechanisms believed to be responsible for the generation of bursts in hydrodynamical systems are reviewed and a new mechanism capable of generating regular or irregular bursts of large dynamic range near threshold is described. The new mechanism is present in the interaction between oscillatory modes of odd and even parity in systems of large but finite aspect ratio, and provides an explanation for the bursting behavior observed in binary fluid convection. Additional applications of the new mechanism are proposed.

1 Introduction

Bursts of activity, be they regular or irregular, are a common occurrence in physical and biological systems. In recent years several models of bursting behavior in hydrodynamical systems have been described using ideas from dynamical systems theory. In this article we review these and then describe a new mechanism (Moehlis & Knobloch [1, 2], Knobloch & Moehlis [3]) which provides an explanation for the bursting behavior observed in experiments on convection in $^3\text{He}/^4\text{He}$ mixtures by Sullivan & Ahlers [4]. This mechanism operates naturally in systems with broken D_4 symmetry undergoing a

Hopf bifurcation from a trivial state. This symmetry, the symmetry group of a square, may be present because of the geometry of the system under consideration (for example, the shape of the container) but also appears in large aspect ratio systems with reflection symmetry (Landsberg & Knobloch [5]). In either case bursting arises as a result of the nonlinear interaction between two nearly degenerate modes with different symmetries.

This article is an expanded version of Knobloch & Moehlis [6].

2 Mechanisms producing bursting

As detailed further below, bursts come in many different forms, distinguished by their dynamic range (i.e., the range of amplitudes during each burst), duration, and recurrence properties. Particularly important for the purposes of the present article is the question of whether the observed bursts occur close to the threshold of a primary instability or whether they are found far from threshold. In the former case a dynamical systems approach is likely to be successful: in this regime the spatial structure usually resembles the eigenfunctions of the linear problem and it is likely that only a small number of degrees of freedom participate in the burst. Such bursts take place fundamentally in the time domain with their spatial manifestation of secondary importance, in contrast to *pulses* which are structures localized in both time *and* space; the latter are not considered here. Since the equations governing the evolution of primary instabilities are often highly symmetric (see Crawford & Knobloch [7]) global bifurcations are likely to occur and these serve as potential candidates for bursting mechanisms. In contrast, bursts found far from threshold usually involve many degrees of freedom but even here some progress is sometimes possible.

2.1 Bursts in the wall region of a turbulent boundary layer

The presence of coherent structures in a turbulent boundary layer is well established (see, e.g., Robinson [8] and the collection of articles

edited by Panton [9]). The space-time evolution of these structures is often characterized by intermittent bursting events involving low speed streamwise “streaks” of fluid. Specifically, let x_1, x_2 , and x_3 be the streamwise, wall normal, and spanwise directions with associated velocity components $U + u_1, u_2$, and u_3 , respectively; here $U(x_2)$ is the mean flow. In a “burst” the streak breaks up and low speed fluid moves upward away from the wall ($u_1 < 0, u_2 > 0$); this is followed by a “sweep” in which fast fluid moves downward towards the wall ($u_1 > 0, u_2 < 0$). After the burst/sweep cycle the streak reforms, often with a lateral spanwise shift.

A low-dimensional model of the burst/sweep cycle was developed by Aubry et al. [10]; further details and later references may be found in Holmes et al. [11, 12]. To construct such a model the authors used a Karhunen-Loève decomposition of the data to identify an energetically dominant empirical set of eigenfunctions, hereafter “modes”. The original study of Aubry et al. [10] used experimental data for pipe flow with $Re \sim 6750$, while later studies used data for channel flow from direct numerical simulation with $Re \sim 3000 - 4000$ and large eddy simulations with $Re \sim 13800$ (Holmes et al. [12]). The model was constructed by projecting the Navier-Stokes equation onto this basis and consists of a set of coupled ODEs for the amplitudes of these modes. The fixed points of these equations are to be associated with the presence of coherent structures. There are two types, related by half-wavelength spanwise translation.

Numerical integration of the model reveals that these fixed points are typically unstable and that they are connected by a heteroclinic cycle. In such a cycle the trajectory alternately visits the vicinities of the two unstable fixed points. In the model of Aubry et al. [10] this heteroclinic cycle is found to be structurally stable, i.e., it persists over a *range* of parameter values. This is a consequence of the $O(2)$ symmetry of the equations inherited from periodic boundary conditions in the spanwise direction. Moreover, for the parameter values of interest this cycle is *attracting*, i.e., it attracts all nearby trajectories. Since the transition from one fixed point to the other corresponds to a spanwise translation by half a wavelength, the re-

current excursions along such a heteroclinic cycle can be identified with the burst/sweep cycle described above. However, since this cycle is attracting, the time between successive bursts will increase as time progresses. This is not observed and Aubry et al. [10] appeal to the presence of a random pressure term modeling the effect of the outer fluid layer to kick the trajectory from the heteroclinic cycle. In the language of Busse [13] such a pressure term results in a *statistical* limit cycle, with the bursting events occurring randomly in time but with a well-defined mean rate. The resulting temporal distribution of the burst events is characterized by a strong exponential tail, matching experimental observations.

Attracting structurally stable heteroclinic cycles occur in a number of problems of this type, i.e., mode interaction problems with $O(2)$ symmetry (Armbruster et al. [14], Proctor & Jones [15], Melbourne et al. [16], Steindl & Troger [17], Krupa [18], Hirschberg & Knobloch [19]).

2.2 Bursts in shear flows undergoing subcritical transition to turbulence

Experimental studies of plane Couette flow and Poiseuille (pipe) flow have shown that at high enough values of the Reynolds number Re the basic laminar flow becomes turbulent. However, these laminar flows are linearly stable at all Re (see, e.g., Drazin & Reid [20]). Consequently, the transition to turbulence in these systems must arise from finite (i.e., not infinitesimal) perturbations to the basic flow; such transitions are called subcritical since the turbulent state exists for values of Re for which the laminar state is stable. Much recent work (reviewed in Baggett & Trefethen [21]) has emphasized the importance of the fact that the linear operators L governing the evolution of perturbations of these flows are non-normal, i.e., $L^\dagger L \neq LL^\dagger$, where L^\dagger is the adjoint of L . Linear systems with a non-normal L can exhibit transient growth even though the laminar state is linearly stable; if the growth is large enough, nonlinearities in the system may then trigger a transition to turbulence. Analysis of low-dimensional models supported by numerical simulations suggests that the mini-

mum perturbation amplitude ϵ that results in turbulence scales as $\epsilon = \mathcal{O}(Re^\alpha)$ for some $\alpha < -1$ (Baggett & Trefethen [21]). Thus, ϵ decreases rapidly with increasing Re , and the experimentally determined Re for transition should be that value at which ϵ is roughly equal to perturbations due to noise or imperfections in the system.

The turbulence excited by finite amplitude perturbations in shear flows often takes the form of turbulent spots which can move, grow, split, and merge (see, e.g., Daviaud et al. [22]). Turbulent spots can also burst intermittently. For example, Bottin et al. [23] observed intermittent turbulent bursts in plane Couette flow for $Re \approx 325$; these bursts were triggered by a spanwise wire through the center of the channel, and could be localized in space by introducing a bead into the central plane. We focus here on this burst-like behavior, also found in low-dimensional models of the subcritical transition to turbulence. The important issue in such models is the attractor to which the flow settles after an appropriate finite perturbation to the basic laminar flow. This will depend crucially on nonlinear terms in the equations, a point emphasized, for example, by Waleffe [24, 25, 26, 27] and Dauchot & Manneville [28]. If this attractor is a fixed point, the system settles into a steady state in which bursts do not occur. On the other hand, if this attractor is a limit cycle it may be appropriate to interpret the resulting behavior as burst-like. This is the case in the model studied in Waleffe [24] in which the amplitudes of streamwise streaks, streamwise rolls, and the streak instability can periodically undergo short-lived explosive growths at the expense of the mean shear. Waleffe [24, 25] refers to this as a self-sustaining process. Since the laminar state is linearly stable, such limit cycles cannot bifurcate off the laminar state. Instead, as pointed out in Waleffe [25, 26], they may be born in a Hopf bifurcation (from a fixed point other than that corresponding to the laminar state) or a homoclinic bifurcation in which a trajectory homoclinic to a fixed point forms at some value of Re such that for smaller (larger) values of Re a limit cycle exists (does not exist), or vice versa. Near such a homoclinic bifurcation, bursts are expected because the trajectory spends a long time near the fixed point, bursting away and return-

ing in a periodic or chaotic fashion, depending on the eigenvalues of the fixed point. Other generic codimension one bifurcations leading to the appearance or disappearance of limit cycles are saddle-node bifurcations of limit cycles and saddle-nodes in which a pair of fixed points appears on the limit cycle (Guckenheimer et al. [29]). Limit cycles could also come in from or go off to infinity. In other models chaotic attractors have been found (see, e.g., Gebhardt & Grossman [30] and Baggett et al. [31]) and these may also give rise to burst-like behavior.

The relation of the bursts described in this section (which occur for moderate values of Re , e.g., $Re \approx 325$) to those which occur in the turbulent boundary layer (which occur for high values of Re) is not completely clear. However, the similarities in the phenomenology have led Waleffe [27] to propose that the self-sustaining process will continue to have importance in the near-wall region of high Re flows.

2.3 Heteroclinic connections to infinity

Another mechanism involving heteroclinic connections, distinct from that discussed in section 2.1, has been investigated by Newell et al. [32, 33] as a possible model for spatio-temporal intermittency in turbulent flow. The authors suggest that such systems may be viewed as nearly Hamiltonian except during periods of localized intense dissipation. A related “punctuated Hamiltonian” approach to the evolution of two-dimensional turbulence has met with considerable success (Carnevale et al. [34] and Weiss & McWilliams [35]). For their description Newell et al. divide the instantaneous states of the flow into two categories, a turbulent soup (TS) characterized by weak coherence, and a singular (S) state characterized by strong coherence, and suppose that the TS and S states are generalized saddles in an appropriate phase space. Furthermore, they suppose that in the Hamiltonian limit the unstable manifold of TS (S) intersects transversally the stable manifold of S (TS). If the constant energy surfaces are noncompact (i.e., unbounded), the evolution of the Hamiltonian system may take the system into regions of phase space with very high (“infinite”) velocities and small scales. These regions are identified

with the S states and high dissipation. In such a scenario the strong dissipation events are therefore identified with excursions along heteroclinic connections to infinity. Perturbations to the system (such as the addition of dissipative processes) may prevent the trajectory from actually reaching infinity, but this underlying unperturbed structure implies that large excursions are still possible.

Newell et al. apply these ideas to the two-dimensional nonlinear Schrödinger equation (NLSE) with perturbations in the form of special driving and dissipative terms which act at large and small scales, respectively. Here S consists of “filament” solutions to the unperturbed NLSE which become singular in finite time and represent coherent structures which may occur at any position in the flow field. When the solution is near S a large portion of the energy is in small scales; for the perturbed equations the dissipative term then becomes important so that the filament solution is approached but collapses before it is reached. This leads to a spatially and temporally random occurrence of localized burst-like events for the perturbed equation. The rate of attraction at S is determined by the faster than exponential rate at which the filament becomes singular, while the rate of repulsion at S is governed by the dissipative process and hence is unrelated to the rate of attraction.

This bursting mechanism shares characteristics with that described in Kaplan et al. [36] in which solutions of a single complex Ginzburg-Landau equation with periodic boundary conditions undergo faster than exponential bursting due to a destabilizing nonlinearity and collapse due to strong nonlinear dispersion (see also Bretherton & Spiegel [37]). A study of a generalization of Burger’s equation modeling nonlocality effects suggests the presence of burst-like events through a similar scenario (Makarenko et al. [38]).

2.4 Bursts in the Kolmogorov flow

The Kolmogorov flow $\mathbf{u} = (k \sin ky, 0)$ is an exact solution of the two-dimensional incompressible Navier-Stokes equation with unidirectional forcing \mathbf{f} at wavenumber k : $\mathbf{f} = (\nu k^3 \sin ky, 0)$. With increasing Reynolds number $Re \equiv \nu^{-1}$ this flow becomes unstable,

and direct numerical simulation with 2π -periodic boundary conditions shows that for moderately high Reynolds numbers and $k > 1$ the resulting flow is characterized by intermittent bursting (She [39], Nicolaenko & She [40, 41, 42, 43], Armbruster et al. [44, 45, 46]). A burst occurs when the system evolves from a coherent vortex-like modulated traveling wave (MW) to a spatially disordered state following transfer of energy from large to small scales. The system then relaxes to the vicinity of another symmetry-related MW state, and the process continues with bursts occurring irregularly but with a well-defined mean period.

The details of what actually happens appear to depend on the value of k because k determines the symmetry of the nonlinear equation describing the evolution of the perturbation streamfunction ϕ about the Kolmogorov flow. Although there is no compelling reason for it, all simulations of this equation have been performed with 2π -periodic boundary conditions in both directions. With these boundary conditions this equation has a symmetry which is the semi-direct product of the dihedral group D_{2k} (generated by the actions $(x, y, \phi) \rightarrow (-x, -y, \phi)$ and $(x, y, \phi) \rightarrow (-x, y + \pi/k, -\phi)$) and the group $SO(2)$ (representing the symmetry under translations $x \rightarrow x + \text{const}$). In the simplest case, $k = 1$, this symmetry group is isomorphic to the direct product of the group $O(2)$ of rotations and reflections of a circle and the group Z_2 representing reflections in the y -direction. Unfortunately, when $k = 1$ the Kolmogorov flow with 2π -periodic boundary conditions is not unstable for any value of Re (Meshalkin & Sinai [47], Green [48], Marchioro [49]), and one is forced to consider $k > 1$. Armbruster et al. [46] analyzed carefully the $k = 2$ case and showed that while a heteroclinic cycle between the MW states does form, it is not structurally stable; the bursts are therefore not produced by a mechanism of the type described in section 2.1. It is possible, however, that the onset of bursting is associated with a symmetry-increasing bifurcation at $Re \equiv Re_s$ (see, e.g., Rucklidge & Matthews [50]). This would explain why the system stays in a single MW state for Re just below Re_s but visits the vicinity of different but symmetry-related MW states for Re just above Re_s . However,

despite much work a detailed understanding of the bursts in this system remains elusive.

An alternative approach is to consider periodic domains with different periodicities in the two directions. In particular, if we consider the domain $\{-\pi < x \leq \pi, -\pi/k < y \leq \pi/k\}$ with $k > 1$ the symmetry group remains $O(2) \times Z_2$ but sufficiently long perturbations now grow. The unstable modes are either even or odd under the reflection $(x, y) \rightarrow (-x, -y)$ with respect to a suitable origin. Mode interaction between these two steady modes can result in a sequence of transitions summarized in figure 1 (Hirschberg & Knobloch [19]): the Kolmogorov flow loses stability to an even mode (Z), followed by a steady state bifurcation to a mixed parity state ($MM_{\pi/2}$). Since each of these states is defined to within a translation in x modulo 2π , we say that it forms a *circle* of states. The $MM_{\pi/2}$ state then loses stability in a further steady state bifurcation to a traveling wave (TW) which in turn loses stability at a Hopf bifurcation to a MW. The MW two-torus terminates in a collision with the two circles of pure parity states, forming an attracting structurally stable heteroclinic cycle connecting them and their quarter-wavelength translates (Hirschberg & Knobloch [19]). In this regime the behavior would resemble that found in the numerical simulations, with higher modes kicking the system away from this cycle. Indeed this sequence of transitions echoes the results obtained by She [39] and Nicolaenko & She [40, 41, 42, 43] for $k = 8$. While it is likely that the $k = 1$ scenario is relevant to these calculations because of the tendency towards an inverse cascade in these two-dimensional systems, we emphasize that, as mentioned above, a careful analysis of the $k = 2$ case by Armbruster et al. [46] shows that while a heteroclinic cycle of the required type does indeed form, it is not structurally stable. The case $k = 4$ has also been studied (Platt et al. [51]) and a similar sequence of transitions found. Undoubtedly simulations on the domain $\{-\pi < x \leq \pi, -\pi/k < y \leq \pi/k\}$ would shed new light on the problem, cf. Posch & Hoover [52].

The group $O(2) \times Z_2$ also arises in convection in rotating straight channels (Knobloch [53]) and in natural convection in a vertical slot

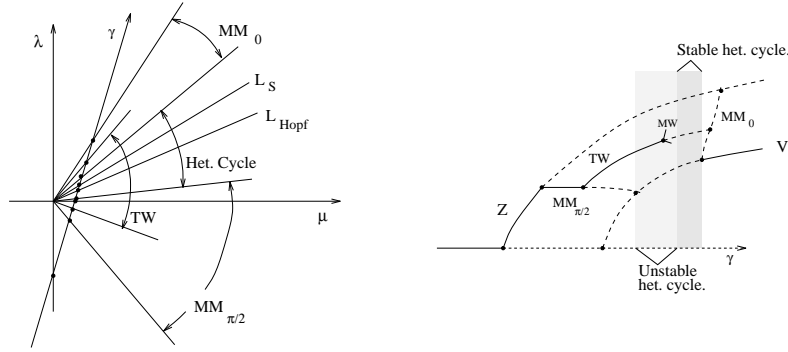


Figure 1: Sample bifurcation diagram for the interaction of an odd and even mode for the Kolmogorov flow obtained by traversing the parameter space along the line γ . A structurally stable heteroclinic cycle exists for a range of parameters. After Hirschberg & Knobloch [19]. Other cuts through parameter space give different bifurcation diagrams.

(Xin et al. [54]). In both of these cases the linear eigenfunctions are either even or odd with respect to a rotation by π and the systems exhibit similar transitions. Related behavior has recently been observed in three-dimensional magnetoconvection with periodic boundary conditions on a square lattice. Unlike the Kolmogorov flow the evolution equation describing a steady state secondary instability of a square pattern is isotropic in the horizontal. Numerical simulations (Rucklidge et al. [55]) show intermittent breakdown of a square pattern followed by its restoration modulo translation.

2.5 Bursts in the Taylor-Couette system

The Taylor-Couette system consists of concentric cylinders enclosing a fluid-filled annulus (see, e.g., Tagg [56]). The cylinders can be rotated independently. In the counterrotating regime the first state consists of spiral vortices of either odd or even parity with respect to midheight. Slightly above onset the flow resembles interpenetrating

spiral (IPS) flow which may be intermittently interrupted by bursts of turbulence which fill the entire flow field (Hamill [57], Coughlin et al. [58, 59]). With periodic boundary conditions in the axial direction numerical simulations by Coughlin et al. [58, 59] show that the IPS flow is temporally chaotic and consists of coexisting modes with different axial and azimuthal wavenumbers. This flow is confined primarily to the vicinity of the inner cylinder where the axisymmetric base flow is subject to an inviscid Rayleigh instability. Coughlin et al. [58, 59] conclude that the onset of turbulence is correlated with a secondary instability of one of the coexisting modes of the IPS flow, namely the basic spiral vortex flow with azimuthal wavenumber $m = 4$. Indeed, when this mode is taken as the initial flow for parameters chosen such that the full IPS flow undergoes bursts, a secondary Hopf bifurcation from this state with the same azimuthal wavenumber but four times the axial wavelength is identified. The secondary instability grows in amplitude and ultimately provides a finite amplitude perturbation to the inviscidly stable flow near the outer cylinder, triggering a turbulent burst throughout the whole apparatus. During a burst small scales are generated throughout the apparatus leading to a rapid collapse of the turbulence and restoration of the IPS flow; the bursting process then repeats roughly periodically in time (see figure 2).

As discussed in section 3.1, in a finite Taylor-Couette apparatus there is a natural mechanism for generating bursts close to onset. This mechanism operates in the regime $\epsilon \sim \Gamma^{-2}$, where ϵ measures the fractional distance above threshold for the primary instability and Γ is the aspect ratio of the annulus (Landsberg & Knobloch [5], Renardy [60]). For larger ϵ the influence of the boundaries no longer extends throughout the apparatus and is confined to boundary layers near the top and bottom. In this regime the dynamics in the bulk may be described by imposing periodic boundary conditions with period that is a multiple of the wavelength of the primary instability. The success of the simulation of the observed turbulent bursts using such periodic boundary conditions (Coughlin et al. [58, 59]) suggests that these bursts occur too far above threshold to be explained by the mechanism described in section 3.1 below. This suggestion is sup-

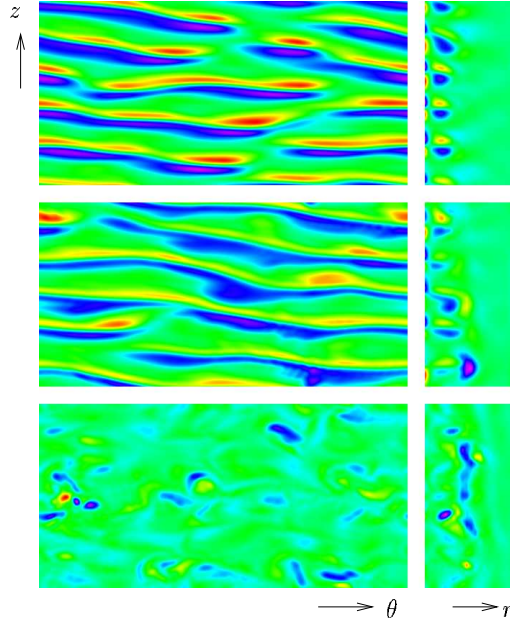


Figure 2: Azimuthal component of vorticity in the laminar interpenetrating spiral state (top), just before a burst (middle), and in the turbulent state (bottom), labeled using polar coordinates. After Coughlin et al. [59]. Courtesy K. Coughlin.

ported by figure 3 which compares the location of the regime where this mechanism may be expected to operate with ϵ_b , the experimental value of ϵ for the onset of bursts, as a function of Γ . The latter is obtained using the approximation $\epsilon_b \approx (R_b - R_{IPS})/R_{IPS}$, where R_{IPS} and R_b are the inner cylinder Reynolds numbers for the onset of IPS flow and bursts, and

$$\begin{aligned}
 R_{IPS} &= (3837 \pm 374)\Gamma^{-1} + 680 \pm 14 \\
 R_b &= (3680 \pm 374)\Gamma^{-1} + 701 \pm 14
 \end{aligned}$$

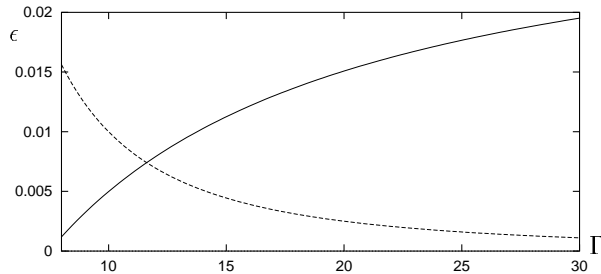


Figure 3: The solid line shows the inner cylinder reduced Reynolds number ϵ_b for the onset of bursts obtained from data in Hamill [57]. The dashed line shows the estimate $\epsilon = \Gamma^{-2}$ near and below which the asymptotic bursting mechanism described in section 3.1 is expected to apply. The bursts found at $\Gamma = 17.9$ and $\Gamma = 26$ (Hamill [57], Coughlin et al. [59]) apparently fall outside the range of validity of the theory of section 3.1.

(Hamill [57]). This is a good approximation for strongly counterrotating cylinders because the IPS flow sets in for inner cylinder Reynolds number only about 1% above the primary onset to spiral vortices (Hamill [57]). The figure suggests that the observed bursts may fall within the range of validity of this theory for Γ only slightly smaller than those used in the experiments ($\Gamma = 17.9, 26$); for such bursts the presence of endwalls should become significant.

2.6 Intermittency

The term intermittency refers to occasional, non-periodic switching between different types of behavior; such transitions may be viewed as bursts. In this section we describe different types of intermittency, dividing them into three classes.

2.6.1 Low-dimensional intermittency

It is often the case that fluid dynamical systems may be modelled by low-dimensional Poincaré maps. Fixed points of such maps correspond to limit cycles of an appropriate dynamical system; when these

lose stability intermittency may result. Without loss of generality we assume that for $\lambda < \lambda_p$ the system is in a “laminar” state corresponding to a stable fixed point of the map, and the onset of intermittency occurs at $\lambda = \lambda_p$. For $\lambda > \lambda_p$ the state of the system will resemble the stable laminar state which existed for $\lambda < \lambda_p$ for some time but will intermittently undergo “bursts” away from this state, followed by “reinjections” to the vicinity of the laminar state. The three types of intermittency identified by Pomeau & Manneville [61] correspond to three different ways in which the laminar state ceases to exist or loses stability at $\lambda = \lambda_p$: Type I intermittency results when a stable and unstable limit cycle annihilate in a saddle-node bifurcation, Type II results when the limit cycle loses stability in a subcritical Hopf bifurcation, while in Type III the limit cycle loses stability in an inverse period-doubling bifurcation. Type I and Type III intermittency have been observed, for example, in Rayleigh-Bénard convection (see Bergé et al. [62] and Dubois et al. [63], respectively), while Type II intermittency has been observed in a hot wire experiment (Ringuet et al. [64]). A different type of intermittency, called Type X, was observed by Price & Mullin [65] in a variant of the Taylor-Couette system; this is similar to Type I intermittency but involves a hysteretic transition due to the nature of the reinjection. Another type of intermittency, called Type V, was introduced in Bauer et al. [66] and He et al. [67]; this is similar in spirit to Type I intermittency but involves one-dimensional maps which are nondifferentiable or discontinuous. These different types of intermittency have distinct properties, such as the scaling behavior of the average time between bursts with $\lambda - \lambda_p$.

2.6.2 Crisis-induced intermittency

A crisis is a sudden change in a strange attractor as a parameter is varied (Grebogi et al. [68, 69, 70]). There are three types of crises, and without loss of generality we assume that the crisis occurs as λ is increased through λ_c . In a boundary crisis, at $\lambda = \lambda_c$ the strange attractor collides with a coexisting unstable periodic orbit which lies on the boundary of the basin of attraction of the strange attractor. This

leads to the destruction of the strange attractor, but chaotic transients will still exist. Intermittency is not associated with this crisis. In an interior crisis the strange attractor collides with a coexisting unstable periodic orbit at $\lambda = \lambda_c$, but here this leads to a widening rather than the destruction of the strange attractor. For λ slightly larger than λ_c the trajectory stays near the region of phase space occupied by the strange attractor before the crisis for long times, but intermittently bursts into a new region. In an attractor merging crisis two strange attractors with basins of attraction separated by a basin boundary are present when $\lambda < \lambda_c$. At λ_c the two strange attractors simultaneously touch the basin boundary and “merge” to form a larger strange attractor for $\lambda > \lambda_c$. Such a crisis is often associated with a symmetry-increasing bifurcation (Chossat & Golubitsky [71]). For $\lambda > \lambda_c$ there is a single strange attractor on which the trajectory intermittently switches between states resembling the distinct strange attractors which existed for $\lambda < \lambda_c$.

2.6.3 Intermittency involving an invariant manifold

A manifold in phase space is invariant if every initial condition on the manifold generates an orbit that remains on the manifold. Invariant manifolds often exist due to symmetries, but this is not necessary. There are several mechanisms for intermittency involving strange attractors on an invariant manifold.

First, suppose that as a bifurcation parameter λ is increased through λ_p , the strange attractor on the invariant manifold loses stability transverse to the manifold; this is called a blowout bifurcation (Ott & Sommerer [72]). Suppose that the dynamics *within* the invariant subspace do not depend on λ . Such a system thus has a skew-product structure (Platt et al. [73]), and λ is called a normal parameter (Ashwin et al. [74]). If the blowout bifurcation is “supercritical” (Ott & Sommerer [72]) then for λ just above λ_p a trajectory will spend a long time near the invariant manifold, intermittently bursting away from it, only to return due to the presence of a reinjection mechanism. This scenario is known as on-off intermittency, where the “off” (“on”) state corresponds to the system

being near (away from) the invariant manifold (see, e.g., Platt et al. [73], Venkataramani et al. [75]). Recently it has been shown that in appropriate circumstances a blowout bifurcation can lead to a structurally stable (possibly attracting) heteroclinic cycle between chaotic invariant sets (Ashwin & Rucklidge [76]).

For systems which lack a skew-product structure and thus are governed by non-normal parameters, in-out intermittency is possible (Ashwin et al. [74], Covas et al. [77]). Here the attraction and repulsion to the invariant subspace are controlled by *different* dynamics. This occurs when the attractor for dynamics restricted to the invariant subspace is smaller than the intersection of the attractor for the full dynamics with the invariant subspace, and may be viewed as a generalization of on-off intermittency in which the attraction to and repulsion from the invariant subspace are controlled by the *same* dynamics.

Another mechanism for bursting occurs when the strange attractor on the invariant manifold attracts typical orbits near the surface but is unstable in the sense that there are unstable periodic orbits embedded within the chaotic set which are transversely repelling. If the trajectory comes near such an unstable periodic orbit, there will be a burst away from the invariant surface. Such bursts may occur intermittently if noise is present or small changes (called “mismatch”) are made to the dynamical system that destroy the invariant surface. The instability of the first of these orbits is known as a bubbling transition (see, e.g., Ashwin et al. [78], Venkataramani et al. [79, 80]).

2.7 Bursts in neural systems

In neural systems, bursting refers to the switching of an observable such as a voltage or chemical concentration between an active state characterized by rapid (spike) oscillations and a rest state. Models of such bursting typically involve singularly perturbed vector fields in which system variables are classified as being “fast” or “slow” depending on whether or not they change significantly over the duration of a single spike. The slow variables may then be thought of as slowly varying parameters for the equations describing the fast

variables (Rinzel [81, 82], Bertram et al. [83], Wang & Rinzel [84], Guckenheimer et al. [29]). As the slow variables evolve, the state of the system in the fast variables may change from a stable periodic orbit (corresponding to the active state) to a stable fixed point (corresponding to the rest state) and vice versa; such transitions are often associated with a region of bistability for the periodic orbit and the fixed point, but need not be. Mechanisms by which such transitions can occur repeatedly have been classified (Rinzel [81, 82], Bertram et al. [83], Wang & Rinzel [84]). Behavior of the time interval between successive spikes near a transition from the active to the rest state is discussed by Guckenheimer et al. [29]; in this paper the presence of a subcritical Hopf-homoclinic bifurcation is also identified as a possible mechanism for the transition from an active to a rest state.

3 A new mechanism for bursting

3.1 Description of the mechanism

We now describe a bursting mechanism which involves the interaction between oscillatory modes in systems with approximate D_4 symmetry, where D_4 is the symmetry group of the square. This mechanism can lead to bursts of large dynamic range very close to the instability onset (Moehlis & Knobloch [1, 2], Knobloch & Moehlis [3]) and is expected to be relevant in many different systems with approximate D_4 symmetry. This symmetry may be present for obvious or subtle reasons, as the following discussion demonstrates.

Consider binary fluid convection in a system of large but finite aspect ratio. If the separation ratio is sufficiently negative the system is overstable, i.e., the primary instability is via a Hopf bifurcation. This is the case for the $^3\text{He}/^4\text{He}$ mixture used by Sullivan & Ahlers [4] in their experiment carried out in a rectangular container $D \equiv \{x, y, z \mid -\frac{1}{2}\Gamma \leq x \leq \frac{1}{2}\Gamma, -\frac{1}{2}\Gamma_y \leq y \leq \frac{1}{2}\Gamma_y, -\frac{1}{2} \leq z \leq \frac{1}{2}\}$ with $\Gamma = 34, \Gamma_y = 6.9$. In this experiment Sullivan & Ahlers observed that immediately above threshold ($\epsilon \equiv (Ra - Ra_c)/Ra_c = 3 \times 10^{-4}$) convective heat transport may take place in a sequence of irregular bursts of large dynamic range despite constant heat input (see figure 4). In

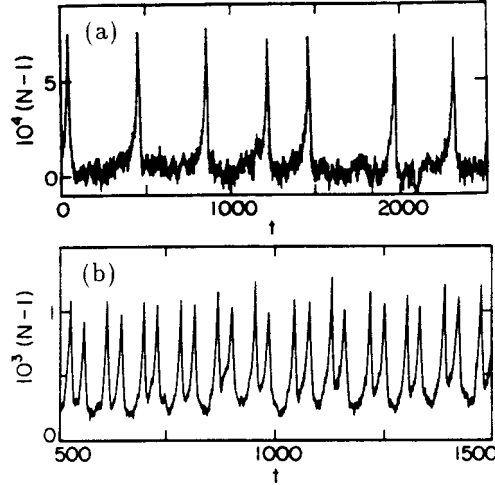


Figure 4: Bursts in binary fluid convection with separation ratio $S = -0.021$. (a) $\epsilon = 3 \times 10^{-4}$, (b) $\epsilon = 3.6 \times 10^{-3}$. The dynamic range of the bursts, measured by the range of $(N - 1)/\epsilon$ where N is the Nusselt number, decreases with increasing ϵ while the burst frequency increases. After Sullivan & Ahlers [4]. Courtesy G. Ahlers.

this system the presence of sidewalls destroys translation symmetry in the x direction which would be present if the system were unbounded, but with identical boundary conditions at the sidewalls the system retains a reflection symmetry about $x = 0$; the primary modes are thus either even or odd with respect to this reflection (Dangelmayr & Knobloch [85]). Numerical simulations of the appropriate partial differential equations suggest that the bursts observed in the experiments involve the interaction between the first odd and even modes of the system (Jacqmin & Heminger [86]; see also Batiste et al. [87] as described in section 3.2). Thus, to describe the dynamical behavior near threshold we suppose that the perturbation from the conduction state takes the form

$$\Psi(x, y, z, t) = \epsilon^{\frac{1}{2}} \text{Re} \{ z_+(t) f_+(x, y, z) + z_-(t) f_-(x, y, z) \} + \mathcal{O}(\epsilon), \quad (1)$$

where $\epsilon \ll 1$, $f_{\pm}(-x, y, z) = \pm f_{\pm}(x, y, z)$.

Following Landsberg & Knobloch [5] we now derive amplitude equations describing the evolution of z_+ and z_- using symmetry arguments. To do this, we first briefly review the topic of bifurcations in systems with symmetry (see, e.g., Golubitsky et al. [88] and Crawford & Knobloch [7]). Suppose that

$$\dot{v} = f(v, \lambda), \tag{2}$$

where $v \in R^n$ and $\lambda \in R^m$ represent dependent variables and system parameters, respectively. Let $\gamma \in G$ describe a linear group action on the dependent variables. We say that if

$$f(\gamma v, \lambda) = \gamma f(v, \lambda) \tag{3}$$

for all $\gamma \in G$ then (2) is *equivariant* with respect to the group G . This is equivalent to the statement that if $v(t)$ is a solution to (2) then so is $\gamma v(t)$. For example, if a system is equivariant under left-right reflections and a right-moving wave exists as a solution, then a reflection-related left-moving wave will also exist as a solution. For the amplitudes z_+ and z_- the requirement that a reflected state (obtained by letting $x \rightarrow -x$ in (1)) also be a state of the system gives the requirement that the amplitude equations be equivariant with respect to the group action

$$\kappa_1 : (z_+, z_-) \rightarrow (z_+, -z_-). \tag{4}$$

Moreover, as argued by Landsberg & Knobloch [5], the equations for the formally infinite system cannot distinguish between the two modes, i.e., in this limit the amplitude equations must also be equivariant with respect to the group action

$$\kappa_2 : (z_+, z_-) \rightarrow (z_-, z_+) \tag{5}$$

which we call an interchange symmetry. These two operations generate together the symmetry group D_4 . For a container with large but finite length, this symmetry will be weakly broken; in particular,

the even and odd modes typically become unstable at slightly different Rayleigh numbers and with slightly different frequencies (see section 3.2). The resulting equations are thus close to those for a 1:1 resonance, but with a special structure dictated by the proximity to D_4 symmetry. Finally, we may put the equations for z_+ and z_- into normal form by performing a series of near-identity nonlinear transformations of the dependent variables so as to simplify the equations as much as possible (see, e.g., Guckenheimer & Holmes [89]). The normal form equations have the additional symmetry (Elphick et al. [90])

$$\hat{\sigma} : (z_+, z_-) \rightarrow e^{i\sigma}(z_+, z_-), \quad \sigma \in [0, 2\pi), \quad (6)$$

which may be interpreted as a phase shift symmetry. Truncating the resulting equations at third order we obtain

$$\begin{aligned} \dot{z}_+ &= [\lambda + \Delta\lambda + i(\omega + \Delta\omega)]z_+ + A(|z_+|^2 + |z_-|^2)z_+ \\ &\quad + B|z_+|^2 z_+ + C\bar{z}_+ z_-^2 \end{aligned} \quad (7)$$

$$\begin{aligned} \dot{z}_- &= [\lambda - \Delta\lambda + i(\omega - \Delta\omega)]z_- + A(|z_+|^2 + |z_-|^2)z_- \\ &\quad + B|z_-|^2 z_- + C\bar{z}_- z_+^2. \end{aligned} \quad (8)$$

Here $\Delta\omega$ measures the difference in frequency between the two modes at onset, and $\Delta\lambda$ measures the difference in their linear growth rates. Under appropriate nondegeneracy conditions (which we assume here) we may neglect all interchange symmetry-breaking contributions to the nonlinear terms. In the following we consider the regime in which λ , $\Delta\lambda$, and $\Delta\omega$ are all of the same order; in the large aspect ratio binary fluid convection context this will occur when these quantities are all $\mathcal{O}(\Gamma^{-2})$ (see section 3.2). We will see that when $\Delta\lambda$ and/or $\Delta\omega$ are nonzero, (7,8) have bursting solutions. Thus, the bursting mechanism may be viewed as an interaction between spontaneous symmetry breaking (in which the trivial conduction state loses stability to a convecting state with less symmetry) and forced symmetry breaking (in which the presence of sidewalls make $\Delta\lambda$ and/or $\Delta\omega$ nonzero, thereby breaking the D_4 symmetry). The introduction of small symmetry-breaking terms is also responsible for the possibility

of complex dynamics in other systems that would otherwise behave in a regular manner (Dangelmayr & Knobloch [91, 85], Lauterbach & Roberts [92], Knobloch [93], Hirschberg & Knobloch [94]).

To identify the bursts we introduce the change of variables

$$z_{\pm} = \rho^{-\frac{1}{2}} \sin\left(\frac{\theta}{2} + \frac{\pi}{4} \pm \frac{\pi}{4}\right) e^{i(\pm\phi+\psi)/2}$$

and a new time-like variable τ defined by $d\tau/dt = \rho^{-1}$. In terms of these variables (7,8) become

$$\frac{d\rho}{d\tau} = -\rho[2A_R + B_R(1 + \cos^2 \theta) + C_R \sin^2 \theta \cos 2\phi] - 2(\lambda + \Delta\lambda \cos \theta)\rho^2 \quad (9)$$

$$\frac{d\theta}{d\tau} = \sin \theta [\cos \theta (-B_R + C_R \cos 2\phi) - C_I \sin 2\phi] - 2\Delta\lambda \rho \sin \theta \quad (10)$$

$$\frac{d\phi}{d\tau} = \cos \theta (B_I - C_I \cos 2\phi) - C_R \sin 2\phi + 2\Delta\omega \rho, \quad (11)$$

where $A = A_R + iA_I$, etc. There is also a decoupled equation for $\psi(t)$ so that fixed points and periodic solutions of equations (9-11) correspond, respectively, to periodic solutions and two-tori in equations (7,8).

In the following we measure the amplitude of the disturbance by $r \equiv |z_+|^2 + |z_-|^2 = \rho^{-1}$; thus $\rho = 0$ corresponds to *infinite* amplitude states. Equations (9-11) show that the restriction to the invariant subspace $\Sigma \equiv \{\rho = 0\}$ is equivalent to taking $\Delta\lambda = \Delta\omega = 0$ in (10,11). The resulting D_4 -symmetric problem has three generic types of fixed points (Swift [95]):

- u solutions with $\cos \theta = 0, \cos 2\phi = 1$
- v solutions with $\cos \theta = 0, \cos 2\phi = -1$
- w solutions with $\sin \theta = 0$.

In the binary fluid context the u , v and w solutions represent mixed parity traveling wave states localized near one of the container walls, mixed parity chevron (or counterpropagating) states, and pure even

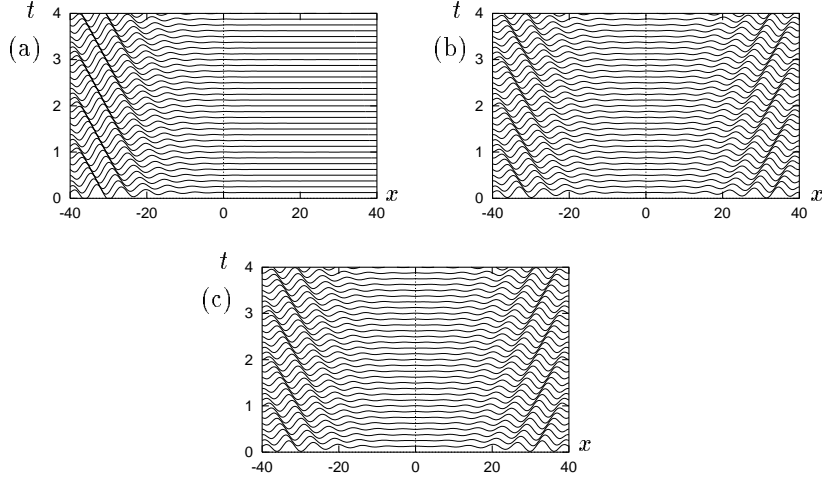


Figure 5: Examples of (a) u , (b) v , (c) w solutions represented in a space-time plot showing the perturbation Ψ from the trivial state.

($\theta = 0$) or odd ($\theta = \pi$) parity chevron states, respectively (Landsberg & Knobloch [5]). Such states are shown in figure 5 using the approximate eigenfunctions

$$f_{\pm}(x) = \left\{ e^{-\gamma x + ix} \pm e^{\gamma x - ix} \right\} \cos \frac{\pi x}{L}, \quad (12)$$

where $\gamma = 0.15 + 0.025i$, $L = 80$ and $-\frac{L}{2} \leq x \leq \frac{L}{2}$. Depending on the coefficients A , B and C the subspace Σ may contain additional fixed points and/or limit cycles (Swift [95]). In our scenario, a burst occurs for $\lambda > 0$ when a trajectory follows the stable manifold of a fixed point (or a limit cycle) $P_1 \in \Sigma$ that is *unstable* within Σ . The instability within Σ then kicks the trajectory towards another fixed point (or limit cycle) $P_2 \in \Sigma$. If this point has an unstable ρ eigenvalue the trajectory escapes from Σ towards a finite amplitude ($\rho > 0$) state, forming a burst. If $\Delta\lambda$ and/or $\Delta\omega \neq 0$ this state may itself be unstable to perturbations of type P_1 and the process then

repeats. This bursting behavior is thus associated with a codimension one heteroclinic cycle between the *infinite amplitude* solutions P_1 and P_2 (Moehlis & Knobloch [2], Knobloch & Moehlis [3]). Examples of such cycles are shown in figure 6. Since in such cycles the trajectory reaches infinity in finite time the heteroclinic cycle actually describes bursts of *finite* duration (Moehlis & Knobloch [2]).

For such a heteroclinic cycle to form it is required that at least one of the branches in the D_4 -symmetric system be subcritical (P_1) and one supercritical (P_2). Based on the $^3\text{He}/^4\text{He}$ experiments, we focus on parameter values for which the u solutions are subcritical and the v, w solutions supercritical when $\Delta\lambda = \Delta\omega = 0$ (Moehlis & Knobloch [1]). When $\Delta\lambda$ and/or $\Delta\omega \neq 0$, two types of oscillations in (θ, ϕ) are possible:

- rotations (see figure 7)
- librations (see figure 8).

For $\lambda > 0$ these give rise, under appropriate conditions, to sequences of large amplitude bursts arising from repeated excursions towards the infinite amplitude ($\rho = 0$) u solutions. Irregular bursts are also readily generated: figure 9 shows bursts arising from chaotic rotations. Figure 10 provides a partial summary of the different solutions of (9-11) and their stability properties; much of the complexity revealed in these figures is due to the Shil'nikov-like properties of the heteroclinic cycle (Moehlis & Knobloch [2], Knobloch & Moehlis [3]).

We now focus on the physical manifestation of the bursts. In figure 11 we show the solutions of figures 7 and 8 in the form of space-time plots using the approximate eigenfunctions (12). The bursts in figure 11(a) are generated as a result of successive visits to *different* (but symmetry-related) infinite amplitude u solutions, cf. figure 7; in figure 11(b) the generating trajectory makes repeated visits to the *same* infinite amplitude u solution, cf. figure 8. The former state is typical of the blinking state identified in binary fluid and doubly diffusive convection in rectangular containers (Kolodner et al. [96], Steinberg et al. [97], Predtechensky et al. [98]). It is likely that the irregular bursts reported in Sullivan & Ahlers [4] are due to such a state. The latter is a new state which we call a *winking* state; winking

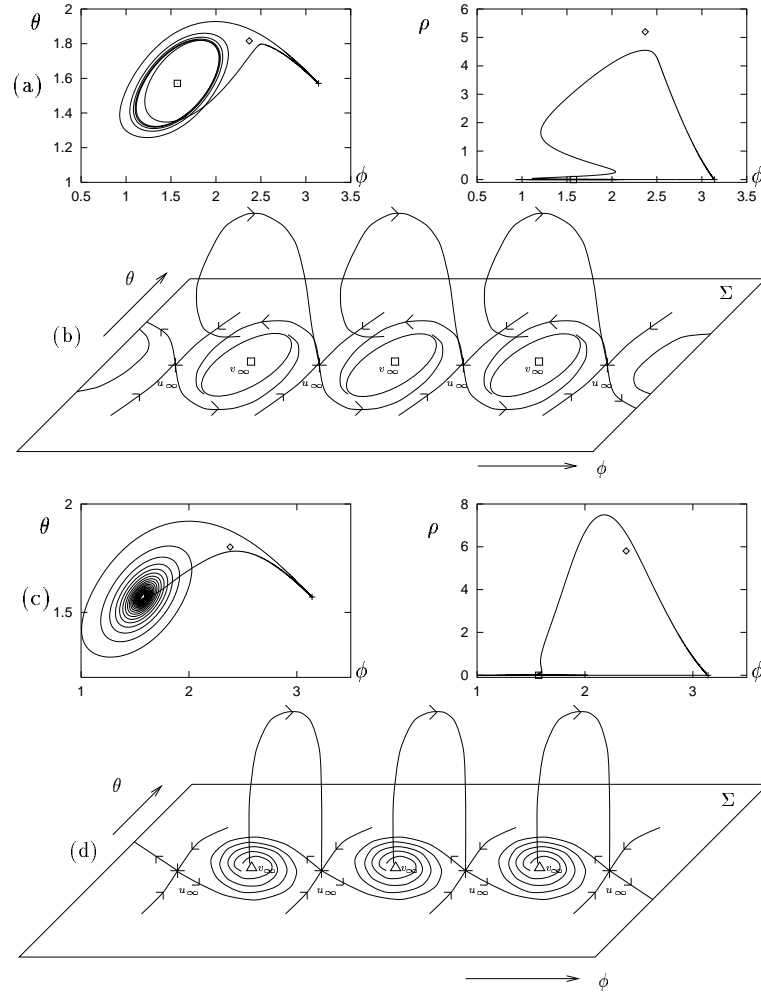


Figure 6: Heteroclinic cycles which exist for $\Delta\lambda = 0.03$, $\Delta\omega = 0.02$, $A = 1 - 1.5i$, $B = -2.8 + 5i$, and (a,b) $C = 1 + i$, $\lambda = 0.0974$, (c,d) $C = 0.9 + i$, $\lambda = 0.08461$. (a) and (c) are obtained numerically, and (b) and (d) sketch the complete heteroclinic networks showing all connections.

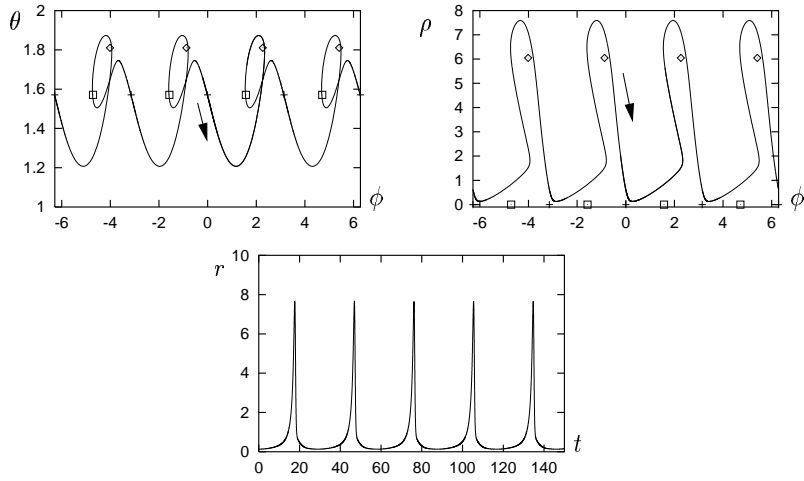


Figure 7: Stable periodic rotations at $\lambda = 0.1$ for $\Delta\lambda = 0.03$, $\Delta\omega = 0.02$, $A = 1 - 1.5i$, $B = -2.8 + 5i$, $C = 1 + i$.

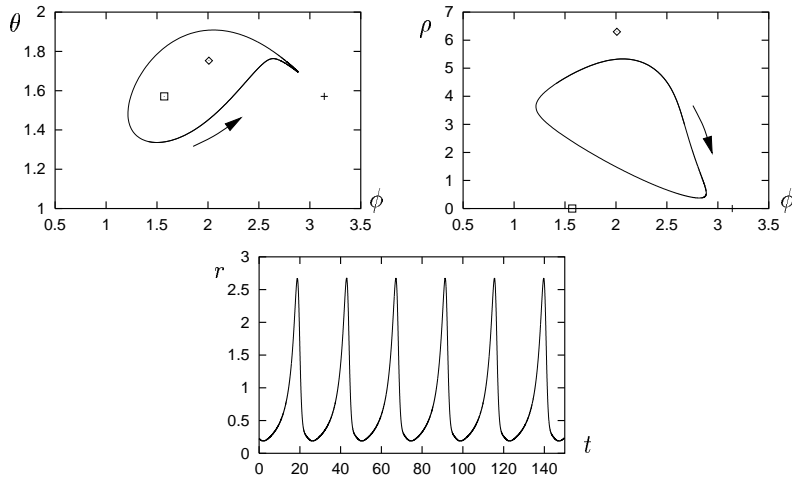


Figure 8: As for figure 7 but showing stable periodic librations at $\lambda = 0.1253$.

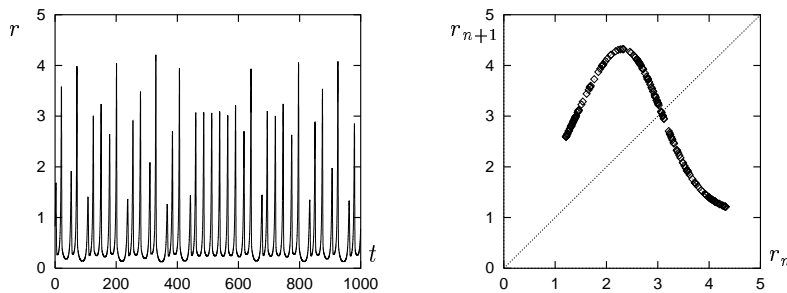


Figure 9: Time series and peak-to-peak plot showing bursts from chaotic rotations with parameters as for figure 7 but with $\lambda = 0.072$.

states may be stable but often coexist with stable chevron-like states which are more likely to be observed in experiments in which the Rayleigh number is ramped upwards (cf. figure 10). For other values of $\Delta\lambda$ and $\Delta\omega$ it is also possible to find stable chaotic winking states and states which are neither purely blinking nor purely winking (see figure 12).

The bursts described above are the result of oscillations in amplitude between two modes of opposite parity and “frozen” spatial structure. Consequently the above burst mechanism applies in systems in which bursts occur very close to threshold. This occurs not only in the convection experiments already mentioned but also in the mathematically identical (counterrotating) Taylor-Couette system where counterpropagating spiral vortices play the same role as traveling waves in convection (Andereck et al. [99], Pierce & Knobloch [100]). In slender systems, such as the convection system described above or a long Taylor-Couette apparatus, a large aspect ratio Γ is required for the presence of the approximate D_4 symmetry. If the size of the D_4 symmetry-breaking terms $\Delta\lambda$, $\Delta\omega$ is increased too much the bursts fade away and are replaced by smaller amplitude, higher frequency states (see figure 13). Indeed, if $\Delta\omega \gg \Delta\lambda$, averaging eliminates the C terms responsible for the bursts (Landsberg & Knobloch [5]). From

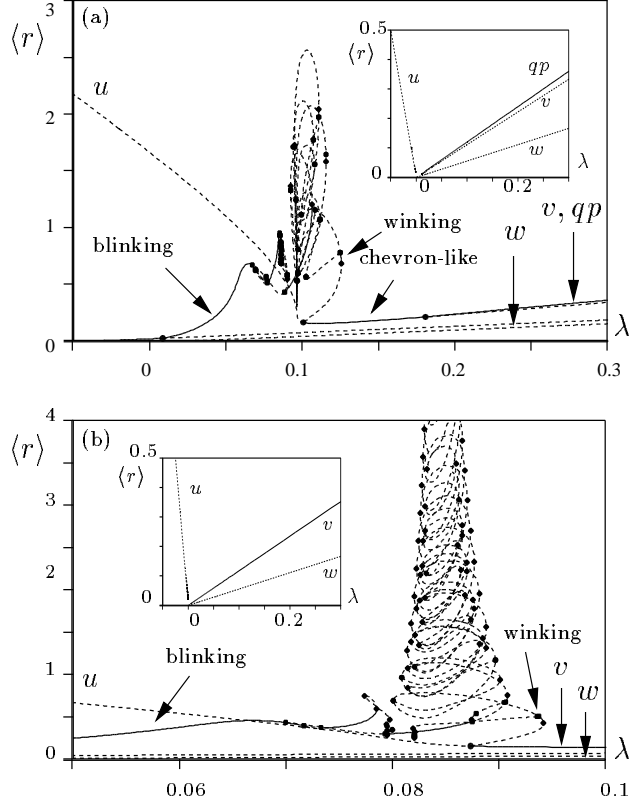


Figure 10: Bifurcation diagrams for (a) $C = 1 + i$ and (b) $C = 0.9 + i$ with $A, B, \Delta\lambda, \Delta\omega$ as in figure 7 showing the time-average of r for different solutions as a function of λ . Solid (dashed) lines indicate stable (unstable) solutions. The branches labeled u, v, w , and qp (quasiperiodic) may be identified in the limit of large $|\lambda|$ with branches in the corresponding diagrams when $\Delta\lambda = \Delta\omega = 0$ (insets). All other branches correspond to bursting solutions which may be blinking or winking states. Circles, squares, and diamonds in the diagram indicate Hopf, period-doubling, and saddle-node bifurcations, respectively.

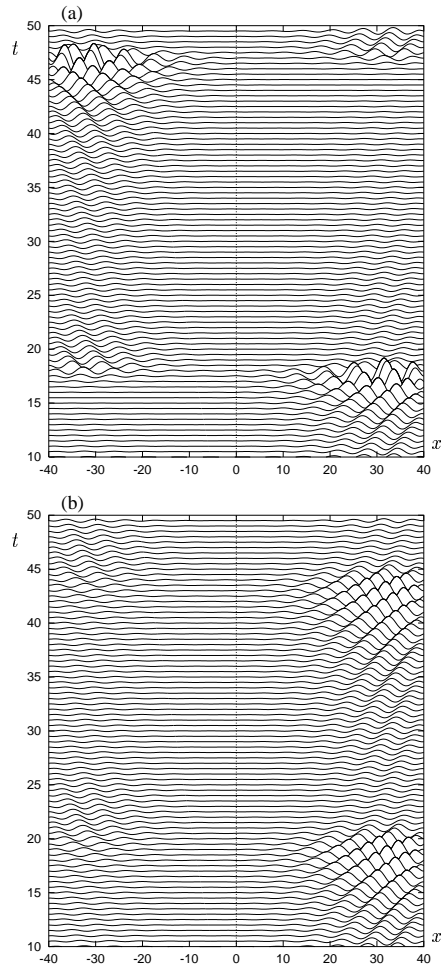


Figure 11: The perturbation Ψ from the trivial state represented in a space-time plot showing (a) a periodic blinking state (in which successive bursts occur at opposite sides of the container) from the trajectory in figure 7, and (b) the periodic winking state (in which successive bursts occur at the same side of the container) for the trajectory in figure 8.

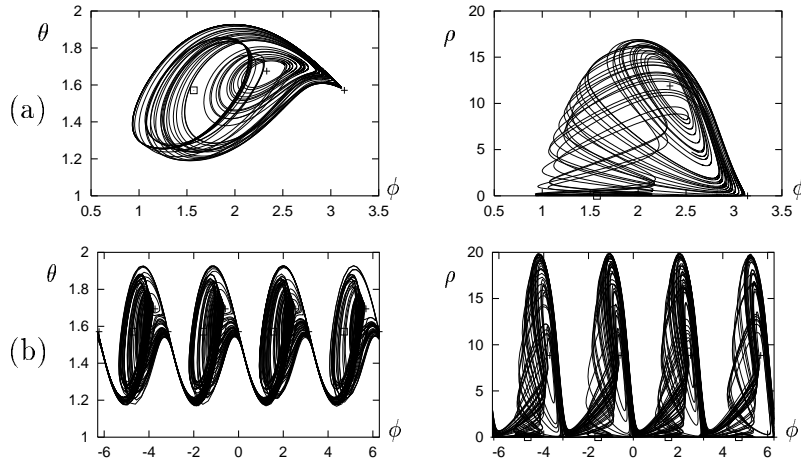


Figure 12: (a) Stable chaotic state with repeated visits to the vicinity of the same infinite amplitude state for $A = 1 - 1.5i$, $B = -2.8 + 5i$, $C = 1 + i$, $\Delta\lambda = 0.03$, $\Delta\omega = -0.02$ and $\lambda = 0.04$, corresponding to a chaotic winking state. (b) Stable chaotic state at $\lambda = 0.03$ with repeated visits to either the same infinite amplitude state or symmetry-related ones. The resulting state is neither purely blinking nor purely winking.

these considerations, we conclude that bursts will not be present if Γ is too small or ϵ too large. However, the mechanism is quite robust and even for $\Delta\omega \gg \Delta\lambda$ it may still be possible to choose λ values so that bursts of large dynamic range occur (Moehlis & Knobloch [2]).

It is possible that the burst amplitude can become large enough for secondary instabilities not captured by the Ansatz (1) to be triggered. Such instabilities could occur on very different scales and result in *turbulent* rather than just large amplitude bursts. However, it should be emphasized that the physical amplitude of the bursts is $\mathcal{O}(\epsilon^{\frac{1}{2}})$ and so approaches zero as $\epsilon \downarrow 0$, cf. eq. (1). Thus despite their large dynamic range (cf. figure 14), the bursts are fully and

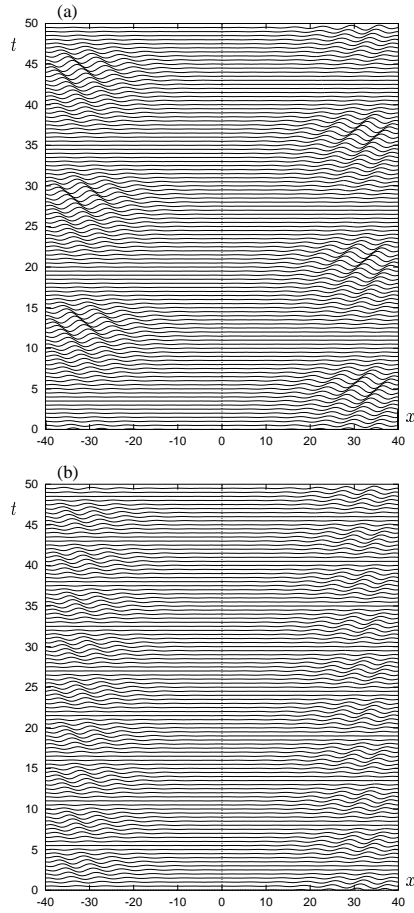


Figure 13: The perturbation Ψ from the trivial state showing stable periodic solutions for the parameters of figure 7 except with (a) $\Delta\omega = 0.1$ and (b) $\Delta\omega = 0.5$. From these and figure 11(a) we see that the bursts fade away with increasing $\Delta\omega$ and are replaced by smaller amplitude, higher frequency states. The amplitude scales are the same here as for figure 11(a).

correctly described by the asymptotic expansion that leads to (7,8). In particular, as shown in Moehlis & Knobloch [2], the mechanism is robust with respect to the addition of small fifth order terms. However, the effects of including D_4 -symmetry-breaking terms in the cubic terms in (7,8) have not been analyzed; these terms can dominate the symmetry-breaking terms retained in the linear terms when ρ is small.

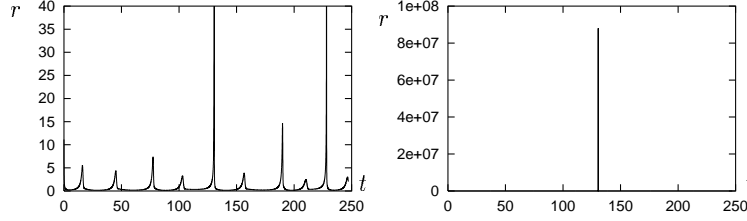


Figure 14: A very large amplitude burst for the parameters of figure 7 except with $\Delta\lambda = 0.06$, $\Delta\omega = -0.01$.

3.2 Applicability to binary mixtures

In view of the motivation for studying systems with approximate D_4 symmetry described above, it is of interest to examine carefully the properties of the linear stability problem for binary fluid convection in finite containers. In the Boussinesq approximation this system is described by the nondimensionalized equations (Clune & Knobloch [101])

$$\partial_t \mathbf{u} + (\mathbf{u} \cdot \nabla) \mathbf{u} = -\nabla P + \sigma R[\theta(1 + S) - S\eta] \hat{\mathbf{z}} + \sigma \nabla^2 \mathbf{u}, \quad (13)$$

$$\partial_t \theta + (\mathbf{u} \cdot \nabla) \theta = w + \nabla^2 \theta, \quad (14)$$

$$\partial_t \eta + (\mathbf{u} \cdot \nabla) \eta = \tau \nabla^2 \eta + \nabla^2 \theta, \quad (15)$$

together with the incompressibility condition

$$\nabla \cdot \mathbf{u} = 0. \quad (16)$$

Here $\mathbf{u} \equiv (u, w)$ is the velocity field in (x, z) coordinates, P , θ and C denote the departures of the pressure, temperature and concentration fields from their conduction profiles, and $\eta \equiv \theta - C$. These equations are to be solved in the rectangular domain $D \equiv \{x, z \mid -\frac{1}{2}\Gamma \leq x \leq \frac{1}{2}\Gamma, -\frac{1}{2} \leq z \leq \frac{1}{2}\}$.

The system is specified by four dimensionless parameters in addition to the aspect ratio Γ : the separation ratio S , the Prandtl and Lewis numbers σ , τ , and the Rayleigh number R . The boundary conditions appropriate to the experiments are no-slip everywhere, with the temperature fixed at the top and bottom and no sideways heat flux. The final set of boundary conditions is provided by the requirement that there is no mass flux through any of the boundaries. The boundary conditions are thus

$$\mathbf{u} = \mathbf{n} \cdot \nabla \eta = 0 \text{ on } \partial D, \quad (17)$$

$$\theta = 0 \text{ at } z = \pm 1/2, \quad \partial_x \theta = 0 \text{ at } x = \pm \Gamma. \quad (18)$$

Here ∂D denotes the boundary of D .

Figure 15 shows the results of solving the *linear* problem describing the stability properties of the conduction state $\mathbf{u} = \theta = \eta = 0$ for parameter values used by Sullivan & Ahlers [4] in their ${}^3\text{He}/{}^4\text{He}$ experiment: $\sigma = 0.6$, $\tau = 0.03$, $\Gamma = 34.0$. The figure shows the neutral stability curves and corresponding frequencies for the first *four* modes in the range $33.0 \leq \Gamma \leq 35.0$ for $S = -0.001$ and $S = -0.021$. Observe that when $|S|$ is sufficiently small the first two families of neutral curves are separated by a gap that is much larger than the amplitude of the “braids” within each family (figure 15(a)). This is typical of what happens in Rayleigh-Bénard convection with non-Neumann boundary conditions (Hirschberg & Knobloch [102]) and makes it easy to justify projecting the fluid equations onto the first two modes that become unstable. However, the situation is not so simple. This is because in the case of overstability this behavior does not persist for all Γ or all values of $|S|$. For larger values of these parameters the results take instead the form shown in figures 15(c,d) which show the linear stability results for $S = -0.021$ and the same range of values of Γ as figures 15(a,b). The modes from the different

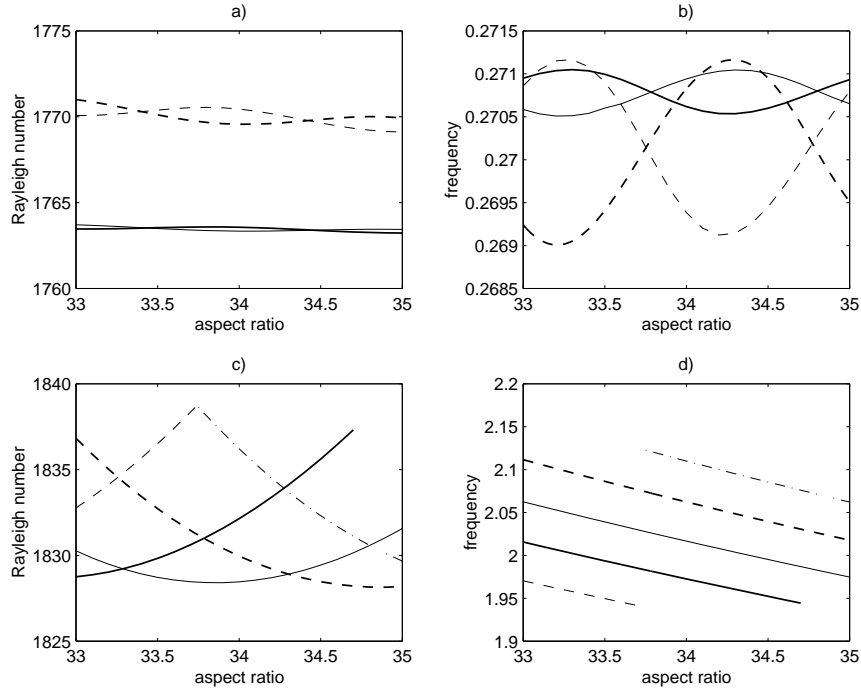


Figure 15: Onset of convection in ${}^3\text{He}/{}^4\text{He}$ mixtures ($\sigma = 0.6$, $\tau = 0.03$) in large aspect ratio containers. (a) Neutral stability curves and (b) corresponding frequencies for the first two even (thick lines) and the first two odd (thin lines) modes as a function of the aspect ratio Γ for $S = -0.001$. (c,d) The same but for $S = -0.021$. Courtesy O. Batiste.

families now cross and the first unstable mode belongs to successively higher and higher families when extrapolated to small $|S|$ (Batiste et al. [87]). Figure 15(c) shows the crossing of two even modes involving a *nonresonant* double Hopf bifurcation (figure 15(d)). As discussed in detail in Batiste et al. [87] the transition between these two types of behavior is mediated by a *resonant* 1:1 mode crossing at a somewhat smaller value of $|S|$. The experimental value of the separation ratio from Sullivan & Ahlers [4], $S = -0.021$, therefore corresponds to the “crossing” case and the projection of the equations onto two modes cannot be rigorously justified except in the neighborhood of mode crossing points.

We denote the growth rates and frequencies of the modes z_{\pm} by λ_{\pm} and ω_{\pm} . For large aspect ratios, the mode frequencies must go like $\omega_{\pm} \sim \omega_{\infty} + c_{1\pm}\Gamma^{-1} + c_{2\pm}\Gamma^{-2} + \dots$. The fact that the frequency curves in figure 15(d) are essentially parallel “straight lines” implies that $c_{1+} \approx c_{1-}$. Therefore, $\Delta\omega \equiv (\omega_+ - \omega_-)/2 = \mathcal{O}(\Gamma^{-2})$ for large Γ (Batiste et al. [87]). Moreover, as argued in Landsberg & Knobloch [5], the parabolic minimum of the neutral stability curve leads to the expectation that $\Delta\lambda = \mathcal{O}(\Gamma^{-2})$. Thus, in the range $\lambda = \mathcal{O}(\Gamma^{-2})$, λ , $\Delta\lambda$, and $\Delta\omega$ are all of the *same* order as $\Gamma \rightarrow \infty$, as required for the applicability of equations (7, 8). Of course, close enough to the mode crossing point $\Delta\lambda \ll \Delta\omega$, and in this region averaging methods can be used to eliminate the $(\bar{z}_+ z_-^2, \bar{z}_- z_+^2)$ terms from the mode interaction equations (Landsberg & Knobloch [5]). However, for typical values of $\Delta\lambda$ it appears likely that the system is correctly described by equations (7, 8), as hypothesized in Landsberg & Knobloch [5] and Moehlis & Knobloch [1].

The first odd and even temperature eigenfunctions for $S = -0.021$ are shown in figure 16 in the form of a space-time diagram, with time increasing upward. As in the approximate expression (12) the eigenfunction consists of waves propagating outwards from the center of the container. The eigenfunction amplitude has a local minimum at the center and increases outwards, peaking near the sidewalls. This type of eigenfunction was anticipated by Cross [103] and is characteristic of eigenfunctions in systems with *positive* group velocity (al-

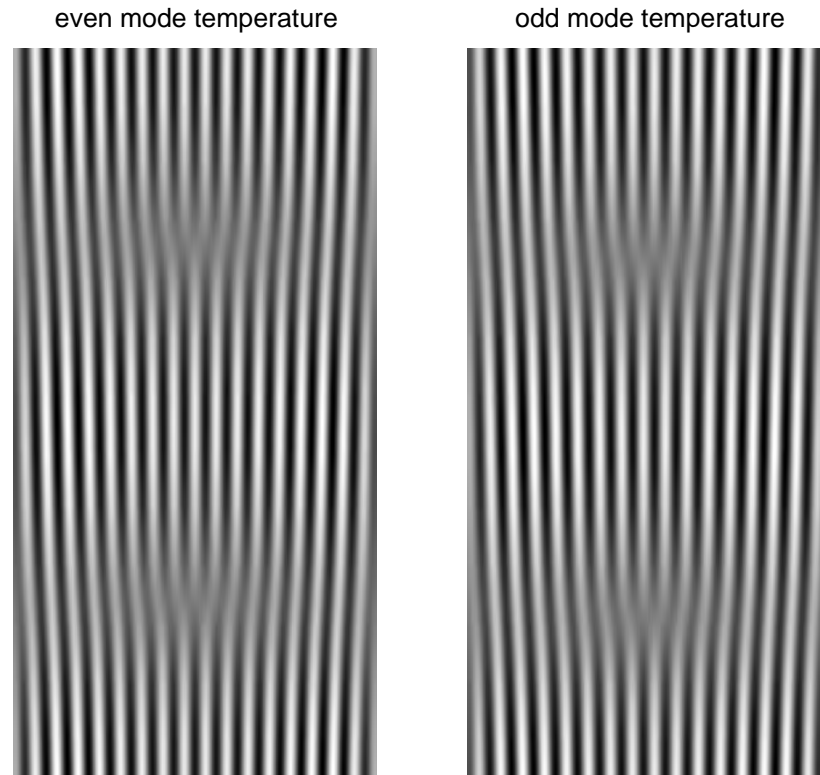


Figure 16: The first even and odd temperature eigenfunctions when $\sigma = 0.6$, $\tau = 0.03$, $\Gamma = 34.0$ and $S = -0.021$ in the form of a space-time plot with time increasing upward. Courtesy O. Batiste.

though, strictly speaking, in a finite system one cannot define a group velocity since the allowed wave number is quantized by the sidewalls as well as being nonuniform). However, for the present purposes the most important observation is that for aspect ratios as large as this, the odd and even eigenfunctions are essentially indistinguishable, as hypothesized by Landsberg & Knobloch [5].

3.3 Other systems with approximate D_4 symmetry

There are a number of other systems of interest where an approximate D_4 symmetry arises in a natural way and the bursting mechanism described in section 3.1 may be relevant. These include overstable convection in small aspect ratio containers with nearly square cross-section (Armbruster [104, 105]) and more generally any partial differential equation on a nearly square domain describing the evolution of an oscillatory instability, cf. Ashwin & Mei [106]. Other systems in which our bursting mechanism might be detected are electrohydrodynamic convection in liquid crystals (Silber et al. [107]; T. Peacock, private communication), lasers (Feng et al. [108]), spring-supported fluid-conveying tubes (Steindl & Troger [109]), and dynamo theories of magnetic field generation in the Sun (Knobloch & Landsberg [110], Knobloch et al. [111]).

Perhaps more interesting is the possibility that large scale spatial modulation due to distant walls may produce bursting in a fully nonlinear state with D_4 symmetry undergoing a symmetry-breaking Hopf bifurcation. As an example we envisage a steady pattern of fully nonlinear two-dimensional rolls. With periodic boundary conditions with period four times the basic roll period, the roll pattern has D_4 symmetry since the pattern is preserved under spatial translations by $1/4$ period and a reflection. If such a pattern undergoes a secondary Hopf bifurcation with a *spatial* Floquet multiplier $\exp i\pi/2$, the Hopf bifurcation breaks D_4 symmetry. If the invariance of the basic pattern under translations by $1/4$ period is only approximate (this would be the case if the roll amplitude varied on a slow spatial scale), the D_4 symmetry itself would be weakly broken and the new mechanism described above could operate.

Also of interest is the Faraday system in a nearly square container. In this system gravity-capillary waves are excited on the surface of a viscous fluid by vertical vibration of the container, usually as a result of a subharmonic resonance. Simonelli & Gollub [112] studied the effect of changing the shape of the container from a square to a slightly rectangular container, focusing on the $(3, 2)$, $(2, 3)$ interaction in this system. These modes are degenerate in a square container and only pure and mixed modes were found in this case. In a slightly rectangular container the degeneracy between these modes is broken, however, and in this case a region of quasiperiodic and chaotic behavior was present near onset. When these oscillations first appear they take the form of relaxation oscillations in which the surface of the fluid remains flat for a long time before a “large wave grows, reaches a maximum, and decays, all in a time short compared with the period”. The duration of the spikes is practically independent of the forcing amplitude, while the interspike period appears to diverge as the forcing amplitude *decreases*. The spikes themselves possess the characteristic asymmetry seen in figures 7 and 8. This behavior occurs when the forcing frequency lies *below* the resonance frequency of the square container, i.e., precisely when D_4 -symmetric problem has a *subcritical* branch. Irregular bursts are also found, depending on parameters, but these are distinct from the chaotic states found by Nagata [113] far from threshold and present even in a square container.

4 Discussion

In this article we have seen that there are many different mechanisms responsible for bursting in hydrodynamical systems. The table below summarizes the different mechanisms described in terms of properties that are most relevant to hydrodynamics. Thus no single mechanism can be expected to provide a universal explanation for all observations. The bursts found experimentally in Taylor-Couette flow (cf. section 2.5) and large aspect ratio binary fluid convection (cf. section 3.1) occur very close to the threshold of a primary instability and

thus have the greatest potential for a successful dynamical systems interpretation of the type emphasized here. We have seen, however, that even for fully developed turbulent boundary layers at very large Reynolds numbers a dynamical systems approach can be profitable (cf. section 2.1).

Although nearly all of the mechanisms we have described rely on the presence of global bifurcations, there are important differences among them. For example, the bursts in the wall region of a turbulent boundary layer described in section 2.1 are due to a (structurally stable) heteroclinic cycle connecting fixed points with *finite* amplitude; such a cycle leads to bursts with a limited dynamic range. In contrast, in the mechanism of section 3.1 the dynamic range is unlimited. Moreover, the role of the fixed points is different: in the former the bursts are associated with the *excursions* between the fixed points while in the latter the bursts are associated *with* the fixed points. Because of the asymptotic stability of the cycle the time between successive bursts in the turbulent boundary layer will increase without bound unless the stochastic pressure term is included; such a stochastic term is not required in the mechanism of section 3.1. In particular, in this mechanism the duration of the bursts remains finite despite the fact that they are associated with a heteroclinic connection. This is because of the faster than exponential escape to “infinity” that is typical of this mechanism. This is so also for the mechanism described in section 2.3. Both of these mechanisms involve global connections to infinity and hence are capable of describing bursts of arbitrarily large dynamic range. The models of the subcritical transition to turbulence and various types of intermittency also produce bursts of finite duration but rely on global reinjection which produces bursts of bounded amplitude.

This work was supported by NSF under grant DMS-9703684 and by NASA under grant NAG3-2152.

section	mechanism	burst recurrence properties	dynamic range
2.1	structurally stable, attracting heteroclinic cycle	increasing period in absence of random pressure force	finite
2.2	periodic orbit near homoclinic bifurcation	periodic or chaotic	finite
2.3	heteroclinic connection to infinity	“random”	unlimited
2.4	symmetry-increasing bifurcation?	irregular but with well-defined mean period	finite
2.5	finite amplitude trigger to inviscidly stable flow from secondary instability	roughly periodic	finite
2.6.1	laminar state ceases to exist or loses stability	chaotic	finite
2.6.2	crisis of strange attractor	chaotic	finite
2.6.3	loss of stability out of invariant manifold	chaotic	finite
2.7	slow variables cause effective change in parameters causing change in state	periodic or chaotic	finite
3.1	heteroclinic cycles involving infinite amplitude states	periodic or chaotic	unlimited

Table 1. The different mechanisms discussed in this article. The term dynamic range refers to the range of amplitudes during each burst.

References

- [1] Moehlis, J. & Knobloch E., Forced symmetry breaking as a mechanism for bursting, *Phys. Rev. Lett.*, **80**, pp. 5329–5332, 1998.
- [2] Moehlis, J. & Knobloch, E., Bursts in oscillatory systems with broken D_4 symmetry, to appear in *Physica D*.
- [3] Knobloch, E. & Moehlis, J., Bursts, *IUTAM Symposium on New Applications of Nonlinear and Chaotic Dynamics in Mechanics*, ed. F.C. Moon, Kluwer, Dordrecht, pp. 51–60, 1999.
- [4] Sullivan, T.S. & Ahlers, G., Nonperiodic time dependence at the onset of convection in a binary liquid mixture, *Phys. Rev. A*, **38**, pp. 3143–3146, 1988.
- [5] Landsberg, A.S. & Knobloch, E., Oscillatory bifurcation with broken translation symmetry, *Phys. Rev. E*, **53**, pp. 3579–3600, 1996.
- [6] Knobloch, E. & Moehlis, J., Bursting mechanisms for hydrodynamical systems, *Pattern Formation in Continuous and Coupled Systems: A Survey Volume*, eds. M. Golubitsky, D. Luss & S.H. Strogatz, Springer, New York, pp. 157–174, 1999.
- [7] Crawford, J.D. & Knobloch, E., Symmetry and symmetry-breaking bifurcations in fluid mechanics, *Ann. Rev. Fluid Mech.*, **23**, pp. 341–387, 1991.
- [8] Robinson, S.K., Coherent motions in the turbulent boundary layer, *Ann. Rev. Fluid Mech.*, **23**, pp. 601–639, 1991.
- [9] *Self-Sustaining Mechanisms of Wall Turbulence*, ed. R.L. Panton, Computational Mechanics Publications, Southampton, 1997.
- [10] Aubry, N., Holmes, P., Lumley, J.L. & Stone, E., The dynamics of coherent structures in the wall region of a turbulent boundary layer, *J. Fluid Mech.*, **192**, pp. 115–173, 1988.

- [11] Holmes, P., Lumley, J.L. & Berkooz, G., *Turbulence, Coherent Structures, Dynamical Systems and Symmetry*, Cambridge University Press, Cambridge, 1996.
- [12] Holmes P.J., Lumley, J.L., Berkooz, G., Mattingly, J.C. & Wittenberg, R.W., Low-dimensional models of coherent structures in turbulence, *Phys. Rep.*, **287**, pp. 337–384, 1997.
- [13] Busse, F.H., Transition to turbulence via the statistical limit cycle route, *Turbulence and Chaotic Phenomena in Fluids*, ed. T. Tatsumi, Elsevier, Amsterdam, pp. 197–202, 1984.
- [14] Armbruster, D., Guckenheimer J. & Holmes, P., Heteroclinic cycles and modulated traveling waves in systems with $O(2)$ symmetry, *Physica D*, **29**, pp. 257–282, 1988.
- [15] Proctor, M.R.E. & Jones, C.A., The interaction of two spatially resonant patterns in thermal convection. Part 1. Exact 2:1 resonance, *J. Fluid Mech.*, **188**, pp. 301–335, 1988.
- [16] Melbourne, I., Chossat, P. & Golubitsky, M., Heteroclinic cycles involving periodic solutions in mode interactions with $O(2)$ symmetry, *Proc. R. Soc. Edinburgh A*, **113**, pp. 315–345, 1989.
- [17] Steindl, A. & Troger, H., Heteroclinic cycles in the three-dimensional postbifurcation motion of $O(2)$ -symmetric fluid conveying tubes, *Appl. Math. Comp.*, **78**, pp. 269–277, 1996
- [18] Krupa, M., Robust heteroclinic cycles, *J. Nonlin. Sci.*, **7**, pp. 129–176, 1997.
- [19] Hirschberg, P. & Knobloch, E., A robust heteroclinic cycle in an $O(2) \times Z_2$ steady-state mode interaction, *Nonlinearity*, **11**, pp. 89–104, 1998.
- [20] Drazin, P.G. & Reid, W.H., *Hydrodynamic Stability*, Cambridge University Press, Cambridge, 1981.

- [21] Baggett, J.S. & Trefethen, L.N., Low-dimensional models of subcritical transition to turbulence, *Phys. Fluids*, **9**, pp. 1043–1053, 1997.
- [22] Daviaud, F., Hegseth, J. & Bergé, P., Subcritical transition to turbulence in plane Couette flow, *Phys. Rev. Lett.*, **69**, pp. 2511–2514, 1992.
- [23] Bottin, S., Dauchot, O. & Daviaud, F., Intermittency in a locally forced plane Couette flow, *Phys. Rev. Lett.*, **79**, pp. 4377–4380, 1997.
- [24] Waleffe, F., Hydrodynamic stability and turbulence: beyond transients to a self-sustaining process, *Stud. Appl. Math.*, **95**, pp. 319–343, 1995.
- [25] Waleffe, F., Transition in shear flows. Nonlinear normality versus non-normal linearity, *Phys. Fluids*, **7**, pp. 3060–3066, 1995.
- [26] Waleffe, F., On a self-sustaining process in shear flows, *Phys. Fluids*, **9**, pp. 883–900, 1997.
- [27] Waleffe, F., How streamwise rolls and streaks self-sustain in a shear flow, *Self-Sustaining Mechanisms of Wall Turbulence*, ed. R.L. Panton, Computational Mechanics Publications, Southampton, pp. 309–332, 1997.
- [28] Dauchot, O. & Manneville, P., Local versus global concepts in hydrodynamic stability theory, *J. Phys. II*, **7**, pp. 371–389, 1997.
- [29] Guckenheimer, J., Harris-Warrick, R., Peck, J. & Willms, A., Bifurcation, bursting, and spike frequency adaptation, *J. Comp. Neuroscience*, **4**, pp. 257–277, 1997.
- [30] Gebhardt, T. & Grossmann, S., Chaos transition despite linear stability, *Phys. Rev. E*, **50**, pp. 3705–3711, 1994.

- [31] Baggett, J.S., Driscoll, T.A. & Trefethen, L.N., A mostly linear model of transition to turbulence, *Phys. Fluids*, **7**, pp. 833–838, 1995.
- [32] Newell, A.C., Rand, D.A. & Russell, D., Turbulent dissipation rates and the random occurrence of coherent events, *Phys. Lett. A*, **132**, pp. 112–123, 1988.
- [33] Newell, A.C., Rand, D.A. & Russell, D., Turbulent transport and the random occurrence of coherent events, *Physica D*, **33**, pp. 281–303, 1988.
- [34] Carnevale, G.F., McWilliams, J.C., Pomeau, Y., Weiss, J.B. & Young, W.R., Evolution of vortex statistics in two-dimensional turbulence, *Phys. Rev. Lett.*, **66**, pp. 2735–2737, 1991.
- [35] Weiss, J.B. & McWilliams, J.C., Temporal scaling behavior of decaying two-dimensional turbulence, *Phys. Fluids A*, **5**, pp. 608–621, 1993.
- [36] Kaplan, E., Kuznetsov, E. & Steinberg, V., Burst and collapse in traveling-wave convection of a binary fluid, *Phys. Rev. E*, **50**, pp. 3712–3722, 1994.
- [37] Bretherton, C.S. & Spiegel, E.A., Intermittency through modulational instability, *Phys. Lett. A*, **96**, pp. 152–156, 1983.
- [38] Makarenko, A.S., Moskalkov, M.N. & Levkov, S.P., On blow-up solutions in turbulence, *Phys. Lett. A*, **235**, pp. 391–397, 1997.
- [39] She, Z.S., Large-scale dynamics and transition to turbulence in the two-dimensional Kolmogorov flow, *Current Trends in Turbulence Research*, eds. H. Branover, M. Mond & Y. Unger, AIAA, Washington, pp. 374–396, 1988.
- [40] Nicolaenko, B. & She, Z.S., Symmetry-breaking homoclinic chaos in Kolmogorov flows, *Nonlinear World, Int. Workshop on Nonlinear and Turbulent Processes in Physics, Kiev 1989* eds. V.G. Bar'yakhtar, V.M. Chernousenko, N.S. Erokhin, A.G.

Sitenko & V.E. Zakharov, World Scientific, Singapore, pp. 602–618, 1990.

- [41] Nicolaenko, B. & She, Z.S., Coherent structures, homoclinic cycles and vorticity explosions in Navier-Stokes flows, *Topological Fluid Mechanics*, ed. H.K. Moffatt, Cambridge University Press, Cambridge, pp. 265–277, 1990.
- [42] Nicolaenko, B. & She, Z.S., Symmetry-breaking homoclinic chaos and vorticity bursts in periodic Navier-Stokes flows, *Eur. J. Mech. B/Fluids*, **10** (no. 2, suppl.), pp. 67–74, 1991.
- [43] Nicolaenko, B. & She, Z.S., Turbulent bursts, inertial sets and symmetry-breaking homoclinic cycles in periodic Navier-Stokes flows, *Turbulence in Fluid Flows: a Dynamical Systems Approach*, eds. G.R. Sell, C. Foias & R. Temam, Springer-Verlag, New York, pp. 123–136, 1993.
- [44] Armbruster, D., Heiland, R., Kostelich, E.J. & Nicolaenko, B., Phase-space analysis of bursting behavior in Kolmogorov flow, *Physica D*, **58**, pp. 392–401, 1992.
- [45] Armbruster, D., Nicolaenko, B., Smaoui, N. & Chossat, P., Analyzing bifurcations in the Kolmogorov flow equations, *Dynamics, Bifurcation and Symmetry*, ed. P. Chossat, Kluwer, Dordrecht, pp. 11–34, 1994.
- [46] Armbruster, D., Nicolaenko, B., Smaoui, N. & Chossat, P., Symmetries and dynamics for 2-D Navier-Stokes flow, *Physica D*, **95**, pp. 81–93, 1996.
- [47] Meshalkin, L.D. & Sinai, Ia.G., Investigation of the stability of a stationary solution of a system of equations for the plane movement of an incompressible viscous fluid, *J. Appl. Math. Mech.*, **25**, pp. 1700–1705, 1961.
- [48] Green, J.S.A., Two-dimensional turbulence near the viscous limit, *J. Fluid Mech.*, **62**, pp. 273–287, 1974.

- [49] Marchioro, C., An example of absence of turbulence for any Reynolds number, *Commun. Math. Phys.*, **105**, pp. 99–106, 1986.
- [50] Rucklidge, A.M. & Matthews, P.C., Analysis of the shearing instability in nonlinear convection and magnetoconvection, *Nonlinearity*, **9**, pp. 311–351, 1996.
- [51] Platt, N., Sirovich, L. & Fitzmaurice, N., An investigation of chaotic Kolmogorov flows, *Phys. Fluids A*, **3**, pp. 681–696, 1991.
- [52] Posch, H.A. & Hoover, W.G., Simulation of two-dimensional Kolmogorov flow with smooth particle applied mechanics, *Physica A*, **240**, pp. 286–296, 1997.
- [53] Knobloch, E., Symmetry and instability in rotating hydrodynamic and magnetohydrodynamic flows, *Phys. Fluids*, **8**, pp. 1446–1454, 1996.
- [54] Xin, S., Le Quéré, P. & Tuckerman, L.S., Bifurcation analysis of double-diffusive convection with opposing thermal and solutal gradients, *Phys. Fluids*, **10**, pp. 850–858, 1998.
- [55] Rucklidge, A.M., Weiss, N.O., Brownjohn, D.P., Matthews, P.C. & Proctor, M.R.E., Compressible magnetoconvection in three dimensions: pattern formation in a strongly stratified layer, preprint, 1999.
- [56] Tagg, R., The Couette-Taylor problem, *Nonlinear Science Today*, **4**, pp. 1–25, 1994.
- [57] Hamill, C.F., Turbulent Bursting in the Couette-Taylor System, MA Thesis, Univ. Texas at Austin, 1995.
- [58] Coughlin, K. & Marcus, P.S., Turbulent bursts in Couette-Taylor flow, *Phys. Rev. Lett.*, **77**, pp. 2214–2217, 1996.
- [59] Coughlin, K., Hamill, C.F., Marcus, P.S. & Swinney, H.L., Turbulent bursts in Couette-Taylor flow, preprint, 1999.

- [60] Renardy, M., A note on bifurcation problems in large containers, *Fluid Dyn. Research*, **24**, pp. 189–199, 1999.
- [61] Pomeau, Y. & Manneville, P., Intermittent transition to turbulence in dissipative dynamical systems, *Commun. Math. Phys.*, **74**, pp. 189–197, 1980.
- [62] Bergé, P., Dubois, M., Manneville, P. & Pomeau, Y., Intermittency in Rayleigh-Bénard convection, *J. Phys. (Paris)*, **41**, pp. L341–345, 1980.
- [63] Dubois, M., Rubio, M.A. & Bergé, P., Experimental evidence of intermitencies associated with a subharmonic bifurcation, *Phys. Rev. Lett.*, **51**, pp. 1446–1449, 1983.
- [64] Ringuet, E., Rozé, C. & Gouesbet, G., Experimental observation of type-II intermittency in a hydrodynamical system, *Phys. Rev. E*, **47**, pp. 1405–1407, 1993.
- [65] Price, T.J. & Mullin, T., An experimental observation of a new type of intermittency, *Physica D*, **48**, pp. 29–52, 1991.
- [66] Bauer, M., Habip, S., He, D.R. & Martienssen, W., New type of intermittency in discontinuous maps, *Phys. Rev. Lett.*, **68**, pp. 1625–1628, 1992.
- [67] He, D.R., Bauer, M., Habip, S., Krueger, U., Martienssen, W. & Wang, B.H., Type V intermittency, *Phys. Lett. A*, **171**, pp. 61–65, 1992.
- [68] Grebogi, C., Ott, E. & Yorke, J.A., Chaotic attractors in crisis, *Phys. Rev. Lett.*, **48**, pp. 1507–1510, 1982.
- [69] Grebogi, C., Ott, E. & Yorke, J.A., Crises, sudden changes in chaotic attractors, and transient chaos, *Physica D*, **7**, pp. 181–200, 1983.
- [70] Grebogi, C., Ott, E., Romeiras, F. & Yorke, J.A., Critical exponents for crisis-induced intermittency, *Phys. Rev. A*, **36**, pp. 5365–5380, 1987.

- [71] Chossat, P. & Golubitsky, M., Symmetry-increasing bifurcations of chaotic attractors, *Physica D*, **32**, pp. 423–436, 1988.
- [72] Ott, E. & Sommerer, J.C., Blowout bifurcations: the occurrence of riddled basins and on-off intermittency, *Phys. Lett. A*, **188**, pp. 39–47, 1994.
- [73] Platt, N., Spiegel, E.A. & Tresser, C., On-Off intermittency: a mechanism for bursting, *Phys. Rev. Lett.*, **70**, pp. 279–282, 1993.
- [74] Ashwin, P., Covas, E. & Tavakol, R., Transverse instability for non-normal parameters, *Nonlinearity*, **12**, pp. 563–577, 1999.
- [75] Venkataramani, S.C., Antonsen Jr., T.M., Ott, E. & Sommerer, J.C., Characterization of on-off intermittent time series, *Phys. Lett. A*, **207**, pp. 173–179, 1995.
- [76] Ashwin, P. & Rucklidge, A.M., Cycling chaos: its creation, persistence and loss of stability in a model on nonlinear magnetoconvection, *Physica D*, **122**, pp. 134–154, 1998.
- [77] Covas, E., Tavakol, R., Ashwin, P., Tworkowski, A. & Brooke, J.M., In-out intermittency in PDE and ODE models of axisymmetric mean-field dynamos, preprint, 1998.
- [78] Ashwin, P., Buescu, J. & Stewart, I., Bubbling of attractors and synchronisation of chaotic oscillators, *Phys. Lett. A*, **193**, pp. 126–139, 1994.
- [79] Venkataramani, S.C., Hunt, B.R., Ott, E., Gauthier, D.J. & Biefang, J.C., Transitions to bubbling of chaotic systems, *Phys. Rev. Lett.*, **77**, pp. 5361–5364, 1996.
- [80] Venkataramani, S.C., Hunt, B.R. & Ott, E., Bubbling transition, *Phys. Rev. E*, **54**, pp. 1346–1360, 1996.
- [81] Rinzel, J., A formal classification of bursting mechanisms in excitable systems, *Proceedings of the International Congress*

of *Mathematicians*, ed. A.M. Gleason, American Mathematical Society, Providence, pp. 1578–1594, 1987.

- [82] Rinzel, J., A formal classification of bursting mechanisms in excitable systems, *Mathematical Topics in Population Biology, Morphogenesis and Neurosciences*, eds. E. Teramoto & M. Yamaguti, Lecture Notes in Biomathematics Vol. 71, Springer-Verlag, Berlin, pp. 267–281, 1987.
- [83] Bertram, R., Butte, M.J., Kiemel, T. & Sherman, A., Topological and phenomenological classification of bursting oscillations, *Bull. Math. Biology*, **57**, pp. 413–439, 1995.
- [84] Wang, X.J. & Rinzel, J., Oscillatory and bursting properties of neurons, *The Handbook of Brain Theory and Neural Networks* ed. M. Arbib, MIT Press, Cambridge, pp. 686–691, 1995.
- [85] Dangelmayr, G. & Knobloch, E., Hopf bifurcation with broken circular symmetry, *Nonlinearity*, **4**, pp. 399–427, 1991.
- [86] Jacqmin, D. & Heminger, J., Double-diffusion with Soret effect in a rectangular geometry: Linear and nonlinear traveling wave instabilities, preprint, 1994.
- [87] Batiste, O., Mercader, I., Net, M. & Knobloch, E., Onset of oscillatory binary fluid convection in finite containers, *Phys. Rev. E*, **59**, pp. 6730–6741, 1999.
- [88] Golubitsky, M., Stewart, I. & Schaeffer, D.G., *Singularities and Groups in Bifurcation Theory, Volume II*, Springer-Verlag, New York, 1988.
- [89] Guckenheimer, J. & Holmes, P., *Nonlinear Oscillations, Dynamical Systems, and Bifurcations of Vector Fields*, Springer-Verlag, New York, 1983.
- [90] Elphick, C., Tirapegui, E., Brachet, M.E., Coulet, P. & Iooss, G., A simple global characterization for normal forms of singular vector fields, *Physica D* **29**, pp. 95–127, 1987.

- [91] Dangelmayr, G. & Knobloch, E., On the Hopf bifurcation with broken $O(2)$ symmetry, *The Physics of Structure Formation*, ed. W. Güttinger & G. Dangelmayr, Springer-Verlag, New York, pp. 387–393, 1987.
- [92] Lauterbach, R. & Roberts, M., Heteroclinic cycles in dynamical systems with broken spherical symmetry, *J. Diff Eq.*, **100**, pp. 22–48, 1992.
- [93] Knobloch, E., System symmetry breaking and Shil’nikov dynamics, *Pattern Formation: Symmetry Methods and Applications*, eds. J. Chadam, M. Golubitsky, W. Langford & B. Wetton, American Mathematical Society, Providence, pp. 271–279, 1996.
- [94] Hirschberg, P. & Knobloch, E., Complex dynamics in the Hopf bifurcation with broken translation symmetry, *Physica D*, **92**, pp. 56–78, 1996.
- [95] Swift, J.W., Hopf bifurcation with the symmetry of the square, *Nonlinearity*, **1**, pp. 333–377, 1988.
- [96] Kolodner, P., Surko, C.M. & Williams, H., Dynamics of traveling waves near the onset of convection in binary fluid mixtures, *Physica D*, **37**, pp. 319–333 (1989).
- [97] Steinberg, V., Fineberg, J., Moses, E. & Rehberg, I., Pattern selection and transition to turbulence in propagating waves, *Physica D*, **37**, pp. 359–383, 1989.
- [98] Predtechensky, A.A., McCormick, W.D., Swift, J.B., Rossberg, A.G. & Swinney, H.L., Traveling wave instability in sustained double-diffusive convection, *Phys. Fluids*, **6**, pp. 3923–3935, 1994.
- [99] Andereck, C.D., Liu, S.S. & Swinney, H.L., Flow regimes in a circular Couette system with independently rotating cylinders, *J. Fluid Mech.*, **164**, pp. 155–183, 1986.

- [100] Pierce, R.D. & Knobloch, E., Spiral vortices in finite cylinders, *Ordered and Turbulent Patterns in Taylor-Couette Flow*, eds. C.D. Andereck & F. Hayot, NATO ASI Series B 297, Plenum, New York, pp. 83–90, 1992.
- [101] Clune, T. & Knobloch, E., Mean flow suppression by endwalls in oscillatory binary fluid convection, *Physica D*, **61**, pp. 106–112, 1992.
- [102] Hirschberg, P. & Knobloch, E., Mode interactions in large aspect ratio convection, *J. Nonlinear Sci.*, **7**, pp. 537–556, 1997.
- [103] Cross, M.C., Traveling and standing waves in binary-fluid convection in finite geometries, *Phys. Rev. Lett.*, **57**, pp. 2943–2946, 1986.
- [104] Armbruster, D., Codimension 2 bifurcation in binary convection with square symmetry, *Nonlinear Evolution of Spatio-Temporal Structures in Dissipative Continuous Systems*, eds. F.H. Busse & L. Kramer, Plenum Press, New York, pp. 385–398, 1990.
- [105] Armbruster, D., Square and almost square symmetry in binary convection, *Eur. J. Mech. B/Fluids*, **10**, (no.2, suppl.), pp. 7–12, 1991.
- [106] Ashwin, P. & Mei, Z., Normal form for Hopf bifurcation of partial differential equations on the square, *Nonlinearity*, **8**, pp. 715–734, 1995.
- [107] Silber, M., Riecke, H. & Kramer, L., Symmetry-breaking Hopf bifurcation in anisotropic systems, *Physica D*, **61**, pp. 260–278, 1992.
- [108] Feng, Q., Moloney, J.V. & Newell, A.C., Transverse patterns in lasers, *Phys. Rev. A*, **50**, pp. R3601–3604, 1994.
- [109] Steindl A. & Troger, H., One and two-parameter bifurcations to divergence and flutter in the three-dimensional motions of a

fluid conveying viscoelastic tube with D_4 symmetry, *Nonlinear Dynam.*, **8**, pp. 161–178, 1995.

- [110] Knobloch, E. & Landsberg, A.S., A new model of the solar cycle, *Mon. Not. R. Astr. Soc.*, **278**, pp. 294–302, 1996.
- [111] Knobloch, E., Tobias, S.M. & Weiss, N.O., Modulation and symmetry changes in stellar dynamos, *Mon. Not. R. Astr. Soc.*, **297**, pp. 1123–1138, 1998.
- [112] Simonelli, F. & Gollub, J.P., Surface wave mode interactions: effects of symmetry and degeneracy, *J. Fluid Mech.*, **199**, pp. 471–494, 1989.
- [113] Nagata, M., Chaotic behaviour of parametrically excited surface waves in square geometry, *Eur. J. Mech. B/Fluids*, **10** (no.2, suppl.), pp. 61–66, 1991.